J. Ind. Geophys. Union, 29(5) (2025), 354-366
https://doi.org/10.71122/JIGU.29(5)2025.0033

Impact of triangular irregularity on the dispersion of SH-waves in a monoclinic crustal layer overlying a dry sandy medium

Tanishqa Shivaji Veer, A. Akilbasha and Vijay Kumar Kalyani*
Department of Mathematics and Statistics
Dr. Vishwanath Karad MIT World Peace University, Pune-411038, Maharashtra, India
*Corresponding author: vijaykumar.kalyani@mitwpu.edu.in

ABSTRACT

In the present paper, a comprehensive study of dispersion characteristics of SH-waves in a monoclinic crustal layer lying over a dry-sandy half-space, with special emphasis on the effect of a triangular irregularity at the interface, has been conducted. We have considered both isotropic and monoclinic layer for the analysis of SH-wave propagation with or without sandiness in the half-space. The governing equations representing equation of motion of SH-waves in a monoclinic medium, is formulated to develop dispersion relation. Further, the results are analyzed and discussed for the variation in various physical parameters such as depth of triangular irregularity, sandiness and the directional dependencies in the monoclinic medium. Moreover, a comparative study has been conducted to assess the extent to which these parameters affect SH-wave propagation differently in monoclinic and isotropic layers. These results are illustrated graphically to highlight the importance of considering interfacial irregularity in seismic wave studies.

Keywords: SH-waves, dispersion, triangular irregularity, monoclinic medium, dry-sandy half-space.

INTRODUCTION

As is well known, SH-waves are seismic waves that move horizontally through the Earth's surface. These waves are particularly useful for studying underground structures as they travel within layered boundaries. It is essential for geophysicists to understand the behavior of such waves in the solids beneath Earth's surface. These solids in the Earth's interior are commonly referred to as minerals or mineral rocks. Minerals with distinct geometric structures are known as crystals. Although crystals can take various forms namely, hexagonal, triclinic, monoclinic, orthorhombic, cubic, tetragonal, and trigonal, nearly one-third of the minerals in the Earth's interior belong to the monoclinic crystalline form. Hence, there is a need to study SH-wave behavior in such media. Several authors have analyzed the dispersion of seismic waves through the monoclinic medium in their studies (Chattopadhyay and Saha, 1996; Kaur and Tomar, 2004). In a related work, Kalyani et al. (2008) presented a model for seismic wave propagation in monoclinic media using the finite difference method. It demonstrated that the anisotropy in the monoclinic medium, hinders the phase velocity of the medium. Sethi and Sharma (2016) discussed the dispersion of SH-waves in a non-homogeneous monoclinic layer over a semi-infinite isotropic medium. Recently, Khan et al. (2021) examined the influence of initial stress on the propagation of SH-waves over a heterogeneous monoclinic half-space. In their work, they studied the variation in the depth of irregularity and non-homogeneity on the phase velocity of the waves. Pradhan et al. (2023) investigated the SH-wave propagation due to a point source at the interface between monoclinic and heterogenous media. They showed that the heterogeneity hinders the phase velocity. Further, Pradhan et al. (2025) extended their study to a two layered structure of functionally graded viscoelastic and monoclinic media, demonstrating the impact of various gradient parameters on dispersion curves, phase velocity, group velocity, and wave number of SH-waves.

The study of seismic waves in the half-space beneath the Earth's crust provides valuable information about the structure of Earth, which plays an important role in the propagation of SH-waves. Although these half-spaces are primarily composed of solid rocks, some may also contain unconsolidated dry sand. Generally, it is observed that SH-waves propagate more slowly through dry sandy media due to energy absorption by the sand grains. Several researchers have considered dry sandy media to study the propagation of seismic waves. For example, Tomar and Kaur (2007) investigated the reflection and transmission of SH-waves at the interface between a dry sandy and an anisotropic half-space. Pal et al. (2016) analyzed the effects of the sandiness parameter and material inhomogeneity on the dispersion of SH-waves propagating through a dry sandy layer, sandwiched between an inhomogeneous isotropic and a homogeneous isotropic half-space. More recently, Madan et al. (2023a) analyzed SH-wave propagation in an orthotropic elastic layer confined between a dry sandy layer and a half-space, highlighting the effect of various parameters on dispersion. Further, in the same year, Madan et al. (2023b) examined Rayleigh waves in an isotropic sandy layer overlying a semi-infinite sandy medium, showing the influence of sandiness on phase velocity.

In earlier studies, different authors in their work assumed interfaces to be perfectly uniform. However, in actual scenarios, geological interfaces are rarely smooth. The Earth's subsurface consists of layered materials with irregularities at the interfaces between different media. The propagation of SH-waves in such layered geological structures is significantly influenced by these geometric irregularities. Numerous studies have examined such irregularities, which affect dispersion of waves with varying layer properties and shapes of the irregularities. Early investigations (Chattopadhyay, 1975; Chattopadhyay and De, 1983) analyzed SH-wave propagation in different media with interfacial irregularities. Kar et al. (1986) studied Love wave propagation in a dry sandy layer having a parabolic irregularity and reported a decrease in phase velocity due to both the sandy medium and the irregular interface. Kalyani and Kar (1986) extended this investigation to anisotropic porous layers sandwiched between two homogeneous half-spaces. They showed that the irregularity at the interface reduces the phase velocity. Further, Chattopadhyay et al. (2008) studied SH-wave propagation in a monoclinic crustal layer lying over an isotropic half-space having a rectangular irregularity at the interface, and found that the depth of the irregularity has a substantial impact on phase velocity of the wave. In a comparative study, Acharya and Roy (2009) analyzed the effects of both parabolic and rectangular irregularities on SH-wave propagation in a magneto-elastic crustal layer. Recently, the effect of rectangular irregularities at the interface on the dispersion of seismic waves has been investigated in different media by several authors, namely Kumar et al. (2015), Gupta et al. (2021), and Kumar and Madan (2022). In a related work, Madan et al. (2024) analyzed Love wave dispersion in a viscoelastic sandy layer over an anisotropic half-space with a parabolic irregularity at the interface, showing the effects of irregularity, sandiness, and dissipation.

Practically, in all these studies, the authors have assumed either parabolic or rectangular irregularities in their models to study SH-wave propagation in different media. However, the present research focuses on triangular irregularity which has significant effect on SH-wave dispersion in such a layered structure. The key focus areas of this study, when the layer is monoclinic, include variations in phase velocity due to the change in (i) the directional dependencies in a monoclinic layer, (ii) depth of triangular irregularities, (iii) the degree of sandiness in the half-space, and (iv) their combined effects. The results of these studies in monoclinic layer have also been compared with the results obtained by assuming the layer to be isotropic and which are also illustrated graphically.

CONCEPT OF CRYSTALLINE MATERIAL

It is a well-known fact that the Earth's crust consists of different minerals having various crystallographic symmetries. Based on their structural arrangements, these crystalline materials are classified into seven crystal systems. Due to their anisotropic nature, these systems influence the seismic wave propagation causing waves to travel at different velocities depending on the crystallographic orientation as a result of their elastic stiffness variations. The stiffness tensors C_{ijkl} capture the anisotropic behavior of these systems with its components constrained by material symmetries. Higher the symmetry of the systems leads to less independent constants resulting in low anisotropy of the material, and lower the symmetry of systems leads to more independent constants resulting in high directional dependency of the material e.g., in cubic system, there are only three independent constants and hence it is isotropic in nature, however, there are twenty-one independent constants in triclinic system and hence it is highly anisotropic. The geometrical properties of the seven crystal systems, along with their stiffness matrices, are presented in Table-1 (Nye, 1985).

Each of these crystal systems, due to their anisotropic characteristics, influence the seismic waves traveling in the Earth's interior. In the present study, a monoclinic medium is considered, where the reduced symmetry with thirteen independent elastic constants results in more complex wave behavior. This model is used to examine the effect of anisotropy on the propagation of SH-waves.

DEVELOPMENT OF THE MODEL

Let us assume a monoclinic crustal layer (M_1) with a triangular irregularity of width $2a$ and depth $h \ll a$ at the interface between the layer and a dry sandy half-space (M_2). The coordinate system is considered with z-axis oriented vertically downwards and x-axis along the interface as illustrated in Figure 1. Let H be the thickness of the monoclinic layer. Additionally, the source generating SH-waves is taken at the depth $d \gg h$ along the z-axis.

Table 1. Geometrical properties of crystals

Crystal system	Edge lengths and angles	Stiffness Matrix
Cubic	$p = q = r$, $\theta = \phi = \gamma = 90^{\circ}$ 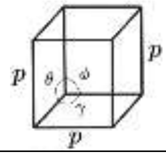	Independent Constants: 3 $\begin{bmatrix} C_{11} & C_{12} & C_{12} & 0 & 0 & 0 \\ C_{12} & C_{11} & C_{12} & 0 & 0 & 0 \\ C_{12} & C_{12} & C_{11} & 0 & 0 & 0 \\ 0 & 0 & 0 & C_{44} & 0 & 0 \\ 0 & 0 & 0 & 0 & C_{44} & 0 \\ 0 & 0 & 0 & 0 & 0 & C_{44} \end{bmatrix}$
Tetragonal	$p = q \neq r$, $\theta = \phi = \gamma = 90°$ 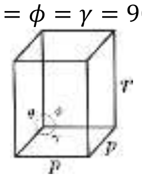	Independent Constants: 6 $\begin{bmatrix} C_{11} & C_{12} & C_{13} & 0 & 0 & 0 \\ C_{12} & C_{11} & C_{13} & 0 & 0 & 0 \\ C_{13} & C_{13} & C_{33} & 0 & 0 & 0 \\ 0 & 0 & 0 & C_{44} & 0 & 0 \\ 0 & 0 & 0 & 0 & C_{44} & 0 \\ 0 & 0 & 0 & 0 & 0 & C_{66} \end{bmatrix}$
Orthorhombic	$p \neq q \neq r$, $\theta = \phi = \gamma = 90°$ 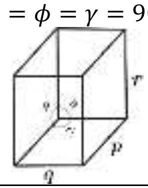	Independent Constants: 9 $\begin{bmatrix} C_{11} & C_{12} & C_{13} & 0 & 0 & 0 \\ C_{12} & C_{22} & C_{23} & 0 & 0 & 0 \\ C_{13} & C_{23} & C_{33} & 0 & 0 & 0 \\ 0 & 0 & 0 & C_{44} & 0 & 0 \\ 0 & 0 & 0 & 0 & C_{55} & 0 \\ 0 & 0 & 0 & 0 & 0 & C_{66} \end{bmatrix}$
Hexagonal	$p = q \neq r$, $\theta = \phi = 90°,\ \gamma = 120°$ 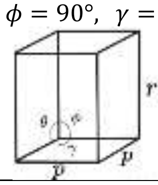	Independent Constants: 5 $\begin{bmatrix} C_{11} & C_{12} & C_{13} & 0 & 0 & 0 \\ C_{12} & C_{11} & C_{13} & 0 & 0 & 0 \\ C_{13} & C_{13} & C_{33} & 0 & 0 & 0 \\ 0 & 0 & 0 & C_{44} & 0 & 0 \\ 0 & 0 & 0 & 0 & C_{44} & 0 \\ 0 & 0 & 0 & 0 & 0 & \frac{C_{11}-C_{12}}{2} \end{bmatrix}$
Trigonal	$p = q = r$, $\theta = \phi = \gamma \neq 90^{\circ}$ 	Independent Constants: 7 $\begin{bmatrix} C_{11} & C_{12} & C_{13} & C_{14} & 0 & 0 \\ C_{12} & C_{11} & C_{13} & -C_{14} & 0 & 0 \\ C_{13} & C_{13} & C_{33} & 0 & 0 & 0 \\ C_{14} & -C_{14} & 0 & C_{44} & 0 & 0 \\ 0 & 0 & 0 & 0 & C_{44} & C_{14} \\ 0 & 0 & 0 & 0 & C_{14} & \frac{C_{11}-C_{12}}{2} \end{bmatrix}$
Monoclinic	$p \neq q \neq r$, $\theta = \gamma = 90°,\ \phi \neq 90°$ 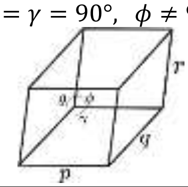	Independent Constants: 13 $\begin{bmatrix} C_{11} & C_{12} & C_{13} & 0 & C_{15} & 0 \\ C_{12} & C_{22} & C_{23} & 0 & C_{25} & 0 \\ C_{13} & C_{23} & C_{33} & 0 & C_{35} & 0 \\ 0 & 0 & 0 & C_{44} & 0 & C_{46} \\ C_{15} & C_{25} & C_{35} & 0 & C_{55} & 0 \\ 0 & 0 & 0 & C_{46} & 0 & C_{66} \end{bmatrix}$
Triclinic	$p \neq q \neq r$, $\theta \neq \phi \neq \gamma \neq 90^{\circ}$ 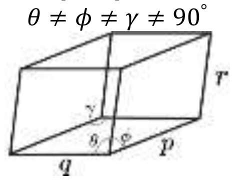	Independent Constants: 21 $\begin{bmatrix} C_{11} & C_{12} & C_{13} & C_{14} & C_{15} & C_{16} \\ C_{12} & C_{22} & C_{23} & C_{24} & C_{25} & C_{26} \\ C_{13} & C_{23} & C_{33} & C_{34} & C_{35} & C_{36} \\ C_{14} & C_{24} & C_{34} & C_{44} & C_{45} & C_{46} \\ C_{15} & C_{25} & C_{35} & C_{15} & C_{55} & C_{56} \\ C_{16} & C_{26} & C_{36} & C_{46} & C_{56} & C_{66} \end{bmatrix}$

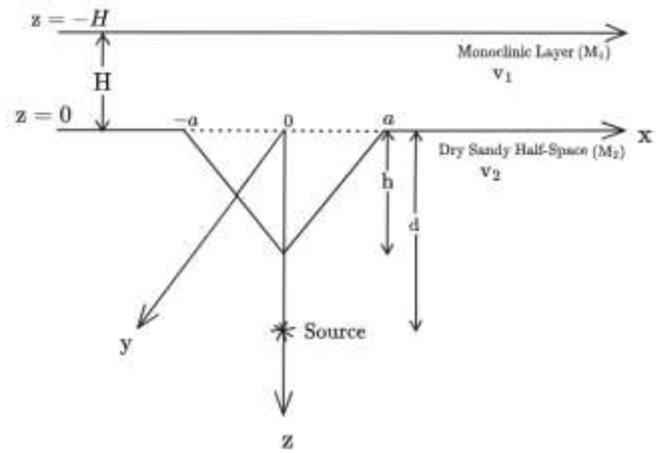

Figure 1. Geometrical description of the model

The geometry of the interface is mathematically represented by:

$$z = \epsilon f(x)$$

Where

$$\mathrm{f(x)} = \begin{cases} \mathrm{h}\left(1 - \dfrac{|\mathrm{x}|}{\mathrm{a}}\right), & \text{for } |\mathrm{x}| \leq \mathrm{a} \\ 0, & \text{for } |\mathrm{x}| > \mathrm{a} \end{cases} \tag{1}$$

in which, $\epsilon = \frac{h}{2a} \ll 1$ serves as the small perturbation parameter.

SH-waves in monoclinic layer

The stress-strain relations for a monoclinic elastic medium with its plane of symmetry normal to the y-axis are expressed as (Pradhan et al., 2023)

$$\begin{bmatrix} T_{xx}^{(1)} \\ T_{yy}^{(1)} \\ T_{zz}^{(1)} \\ T_{yz}^{(1)} \\ T_{xz}^{(1)} \\ T_{xy}^{(1)} \end{bmatrix} = \begin{bmatrix} C_{11} & C_{12} & C_{13} & 0 & C_{15} & 0 \\ C_{12} & C_{22} & C_{23} & 0 & C_{25} & 0 \\ C_{13} & C_{23} & C_{33} & 0 & C_{35} & 0 \\ 0 & 0 & 0 & C_{44} & 0 & C_{46} \\ C_{15} & C_{25} & C_{35} & 0 & C_{55} & 0 \\ 0 & 0 & 0 & C_{46} & 0 & C_{66} \end{bmatrix} \begin{bmatrix} S_1 \\ S_2 \\ S_3 \\ S_4 \\ S_5 \\ S_6 \end{bmatrix} \tag{2}$$

where, $T_{xx}^{(1)}, T_{yy}^{(1)}, T_{zz}^{(1)}, \ldots$ denote the stress components of stress tensor, $C_{kj}(k, j = 1,2, \ldots, 6)$ are the elastic coefficients and $S_k(k = 1,2, \ldots, 6)$ are the strain-displacement relations defined as

$$S_1 = \frac{\partial u_1}{\partial x}, S_2 = \frac{\partial v_1}{\partial y}, \quad S_3 = \frac{\partial w_1}{\partial z}, \quad S_4 = \frac{\partial w_1}{\partial y} + \frac{\partial v_1}{\partial z}, \quad S_5 = \frac{\partial u_1}{\partial z} + \frac{\partial w_1}{\partial x}, \quad S_6 = \frac{\partial v_1}{\partial x} + \frac{\partial u_1}{\partial y}. \tag{3}$$

In the absence of body forces, the equations of motion are given by

$$\left.\begin{aligned} \frac{\partial T_{xx}^{(1)}}{\partial x} + \frac{\partial T_{xy}^{(1)}}{\partial y} + \frac{\partial T_{xz}^{(1)}}{\partial z} = \rho_1 \frac{\partial^2 u_1}{\partial t^2}, \\ \frac{\partial T_{yx}^{(1)}}{\partial x} + \frac{\partial T_{yy}^{(1)}}{\partial y} + \frac{\partial T_{yz}^{(1)}}{\partial z} = \rho_1 \frac{\partial^2 v_1}{\partial t^2}, \\ \frac{\partial T_{zx}^{(1)}}{\partial x} + \frac{\partial T_{zy}^{(1)}}{\partial y} + \frac{\partial T_{zz}^{(1)}}{\partial z} = \rho_1 \frac{\partial^2 w_1}{\partial t^2}, \end{aligned}\right\} \tag{4}$$

where ρ_1 is the density of the monoclinic layer M_1. Here, the subscript and superscript '1' indicate monoclinic layer M_1.

Considering SH-waves traveling in the positive direction of x-axis and polarised in y-direction, we have

$$u = 0, \qquad v = v(x, z, t), \qquad w = 0. \tag{5}$$

Substituting Eqs. (3) and (5) in Eq. (2), the stress-strain relations reduce to

$$T_{xx}^{(1)} = T_{yy}^{(1)} = T_{zz}^{(1)} = T_{xz}^{(1)} = 0, \quad T_{yz}^{(1)} = C_{44} \frac{\partial v_1}{\partial z} + C_{46} \frac{\partial v_1}{\partial x}, \quad T_{xy}^{(1)} = C_{46} \frac{\partial v_1}{\partial z} + C_{66} \frac{\partial v_1}{\partial x}. \tag{6}$$

Substituting Eq. (6) into Eq. (4), the propagation of SH-waves in the monoclinic layer obtained as

$$C_{66} \frac{\partial^2 v_1}{\partial x^2} + 2C_{46} \frac{\partial^2 v_1}{\partial x \partial z} + C_{44} \frac{\partial^2 v_1}{\partial z^2} = \rho_1 \frac{\partial^2 v_1}{\partial t^2}. \tag{7}$$

Using the time harmonic solution,

$$v_1 = V_1(x, z) e^{i\omega t},$$

in Eq. (7), we get

$$C_{66} \frac{\partial^2 V_1}{\partial x^2} + 2C_{46} \frac{\partial^2 V_1}{\partial x \partial z} + C_{44} \frac{\partial^2 V_1}{\partial z^2} + \omega^2 \rho_1 V_1 = 0, \tag{8}$$

where ω represents the angular frequency.

The Fourier and inverse Fourier transform of $V_1(x,z)$ is given by (Kreyszig, 2006):

$$\left.\begin{aligned} \bar{V}_1(\zeta,z) &= \int_{-\infty}^{\infty} V_1(x,z)e^{i\zeta x}dx, \\ V_1(x,z) &= \frac{1}{2\pi}\int_{-\infty}^{\infty} \bar{V}_1(\zeta,z)e^{-i\zeta x}d\zeta. \end{aligned}\right\} \quad (9)$$

Applying the above defined Fourier transform to Eq. (8), we have

$$C_{44}\frac{d^2\bar{V}_1}{dz^2} - 2i\zeta C_{46}\frac{\bar{V}_1}{dz} + (\omega^2\rho_1 - \zeta^2 C_{66})\bar{V}_1 = 0. \quad (10)$$

Therefore, the solution of Eq. (10) is

$$\bar{V}_1 = e^{-\frac{s}{2}z}(A\cos p_1 z + B\sin p_1 z), \quad (11)$$

where A and B are arbitrary constants, and

$$s = -\frac{2i\zeta C_{46}}{C_{44}}, \quad p_1 = \sqrt{\frac{\omega^2}{\beta_1^2} - \zeta^2\frac{C_{66}}{C_{44}} + \zeta^2\frac{C_{46}^2}{C_{44}^2}}, \quad \beta_1 = \sqrt{\frac{C_{44}}{\rho_1}}. \quad (12)$$

By taking the inverse Fourier transform of Eq. (11), the displacement of SH-wave propagation in the monoclinic medium is given by

$$V_1(x,z) = \frac{1}{2\pi}\int_{-\infty}^{\infty} e^{-\frac{s}{2}z}(A\cos p_1 z + B\sin p_1 z)e^{-i\zeta x}d\zeta. \quad (13)$$

SH-waves in dry sandy half-space

The stress-strain relations for a dry sandy half-space are expressed as (Pal, 1985)

$$\left.\begin{aligned} T_{xx}^{(2)} &= (\lambda + 2\mu_2)u_2 + \lambda v_2 + \lambda w_2, \\ T_{yy}^{(2)} &= \lambda u_2 + (\lambda + 2\mu_2)v_2 + \lambda w_2, \\ T_{zz}^{(2)} &= \lambda u_2 + \lambda v_2 + (\lambda + 2\mu_2)w_2, \\ T_{yz}^{(2)} &= \mu_2(w_2 + v_2), \\ T_{zx}^{(2)} &= \mu_2(u_2 + w_2), \\ T_{xy}^{(2)} &= \mu_2(u_2 + v_2), \end{aligned}\right\} \quad (14)$$

where, λ is the Lame parameter and μ_2 is the rigidity of the dry sandy half-space given by

$$\mu_2 = \frac{\mu_0}{\eta},$$

where η represents the sandiness parameter and μ_0 denotes the rigidity of the classical elastic medium. The superscript and subscript '2' indicate dry sandy half-space M_2.

Similarly, the equation of motion for propagation of SH-waves in the lower dry sandy half-space is given by (Kar et al., 1986)

$$\frac{\partial^2 v_2}{\partial x^2} + \frac{\partial^2 v_2}{\partial z^2} = \frac{1}{\beta_2^2}\frac{\partial^2 v_2}{\partial t^2}, \quad (15)$$

where, β_2 represents the speed of the SH-waves in the dry sandy semi-infinite medium, defined by:

$$\beta_2 = \frac{1}{\sqrt{\eta}}\beta_2'$$

in which,

$$\beta_2' = \sqrt{\frac{\mu_0}{\rho_2}}$$

where ρ_2 denotes the density of the dry sandy half-space.

Using the time harmonic solution,

$$v_2 = V_2(x,z)e^{i\omega t},$$

in Eq. (15), we get

$$\frac{\partial^2 V_2}{\partial x^2} + \frac{\partial^2 V_2}{\partial z^2} + \eta\frac{\omega^2}{\beta_2'^2}V_2 = 0. \quad (16)$$

Applying the Fourier transform defined in Eq. (9) to Eq. (16), we get

$$\frac{d^2\bar{V}_2}{dz^2} - \left(\zeta^2 - \eta\frac{\omega^2}{\beta_2'^2}\right)\bar{V}_2 = 0. \quad (17)$$

Thus, the solution of Eq. (17) is:

$$\bar{V}_2 = Ce^{-p_2 z} \quad (18)$$

where C is the arbitrary constants, and

$$p_2 = \sqrt{\zeta^2 - \eta\frac{\omega^2}{\beta_2'^2}}. \quad (19)$$

By taking the inverse Fourier transform of Eq. (18), the displacement of SH-wave propagation in the dry sandy half-space is given by

$$V_2(x,z) = \frac{1}{2\pi}\int_{-\infty}^{\infty}\left(Ce^{-p_2 z} + \frac{2}{p_2}e^{p_2 z}e^{-p_2 d}\right)e^{-i\zeta x}d\zeta, \quad (20)$$

where the second term in Eq. (20) for V_2 arises due to the contribution of the source in the lower medium (Pilant, 1979).

Boundary conditions

Since a monoclinic layer lies over a dry sandy semi-infinite medium, the boundary conditions:

(A) at the interface $z = \epsilon f(x)$ are:

(i) displacements are continuous:

$$v_1 = v_2 \tag{21}$$

(ii) shear stresses are continuous:

$$T_{yz}^{(1)} = T_{yz}^{(2)},$$

which gives,

$$C_{44}\frac{\partial v_1}{\partial z} + C_{46}\frac{\partial v_1}{\partial x} - \epsilon f'(x)\left(C_{46}\frac{\partial v_1}{\partial z} + C_{66}\frac{\partial v_1}{\partial x}\right) = \frac{\mu_0}{\eta}\left(\frac{\partial v_2}{\partial z} - \epsilon f'(x)\frac{\partial v_2}{\partial x}\right) \tag{22}$$

(B) at the upper boundary $z = -H$,

shear stress vanishes, we have

$$T_{yz}^{(1)} = 0,$$

which gives,

$$C_{44}\frac{\partial v_1}{\partial z} + C_{46}\frac{\partial v_1}{\partial x} = 0, \tag{23}$$

where, $f'(x) = \frac{df(x)}{dx}$.

For the irregular interface, A, B, and C are the functions of ϵ. Expanding them in the increasing powers of small ϵ and retaining terms up to first order, we have:

$$\begin{aligned} &A \cong A_0 + \epsilon A_1, \quad B \cong B_0 + \epsilon B_1, \quad C \cong C_0 + \epsilon C_1, \\ &e^{\pm g\epsilon f} \cong 1 \pm g\epsilon f, \quad cos(p_1\epsilon f) \cong 1, \quad sin(p_1\epsilon f) \cong p_1\epsilon f \end{aligned} \tag{24}$$

where, g is any quantity.

Using Eq. (24), the boundary conditions (21), (22), and (23) reduces to

$$\begin{aligned} &(A_0 + \epsilon A_1)\left[C_{44}p_1 \sin p_1 H - C_{44}\frac{s}{2}\cos p_1 H - i\zeta C_{46}\cos p_1 z\right] \\ &+(B_0 + \epsilon B_1)\left[C_{44}p_1 \cos p_1 H + C_{44}\frac{s}{2}\sin p_1 H + i\zeta C_{46}\sin p_1 z\right] = 0 \end{aligned} \tag{25}$$

$$\epsilon\int_{-\infty}^{\infty}\left(A_0\frac{s}{2} - B_0 p_1 - C_0 p_2 + 2e^{-dp_2}\right) f(x) e^{-i\zeta x} d\zeta = \int_{-\infty}^{\infty}\left[A_0 - C_0 - \frac{2}{p_2}e^{-p_2 d} + \epsilon(A_1 - C_1)\right] e^{-i\zeta x} d\zeta, \tag{26}$$

and,

$$\begin{aligned} &\epsilon\int_{-\infty}^{\infty}\Bigg\{\Bigg[C_{44}\left(-A_0p_1^2 - sp_1B_0 + \frac{s^2}{4}A_0\right) - i\zeta C_{46}\left(p_1B_0 - \frac{s}{2}A_0\right) - \frac{\mu_0}{\eta}\left(C_0p_2^2 + 2p_2e^{-p_2d}\right)\Bigg] f(x) \\ &+\left[-C_{46}\left(p_1B_0 - \frac{s}{2}A_0\right) + i\zeta C_{66}A_0 - i\zeta\frac{\mu_0}{\eta}\left(C_0 + \frac{2}{p_2}e^{-p_2d}\right)\right] f'(x)\Bigg\} e^{-i\zeta x} d\zeta \\ &= -\int_{-\infty}^{\infty}\Bigg[C_{44}\left(p_1B_0 - \frac{s}{2}A_0\right) + p_2\frac{\mu_0}{\eta}C_0 - 2\frac{\mu_0}{\eta}e^{-p_2d} \\ &+\epsilon\left(C_{44}p_1B_1 - C_{44}\frac{s}{2}A_1 - i\zeta C_{46}A_1 + p_2\frac{\mu_0}{\eta}C_1\right) - i\zeta C_{46}A_0\Bigg] e^{-i\zeta x} d\zeta, \end{aligned} \tag{27}$$

respectively.

DEVELOPMENT OF DISPERSION RELATION

To develop dispersion relation of SH-wave propagation in a monoclinic layer over a dry sandy half-space, we use Fourier and inverse Fourier transform of $f(x)$ defined as (Kreyszig, 2006)

$$\left.\begin{aligned} \bar{f}(\xi) &= \int_{-\infty}^{\infty} f(x)e^{i\xi x}dx, \\ f(x) &= \frac{1}{2\pi}\int_{-\infty}^{\infty}\bar{f}(\xi)e^{-i\xi x}dx. \end{aligned}\right\} \tag{28}$$

Applying the Fourier transform given in Eq. (28) to Eqs. (26) and (27), we get

$$\begin{aligned} &\frac{\epsilon}{2\pi}\int_{-\infty}^{\infty}\int_{-\infty}^{\infty}\left(A_0\frac{s}{2} - B_0p_1 - C_0p_2 + 2e^{-dp_2}\right)\bar{f}(\xi)e^{-i(\zeta+\xi)x}d\xi d\zeta \\ &= \int_{-\infty}^{\infty}\left[A_0 - C_0 - \frac{2}{p_2}e^{-p_2d} + \epsilon(A_1 - C_1)\right]e^{-i\zeta x}d\zeta, \end{aligned} \tag{29}$$

and,

$$\begin{aligned} &\frac{\epsilon}{2\pi}\int_{-\infty}^{\infty}\int_{-\infty}^{\infty}\Bigg\{\Bigg[C_{44}\left(-A_0p_1^2 - sp_1B_0 + \frac{s^2}{4}A_0\right) - i\zeta C_{46}\left(p_1B_0 - \frac{s}{2}A_0\right) - \frac{\mu_0}{\eta}\left(C_0p_2^2 + 2p_2e^{-p_2d}\right)\Bigg] \\ &+\left[i\xi C_{46}\left(p_1B_0 - \frac{s}{2}A_0\right) + \zeta\xi C_{66}A_0 - \zeta\xi\frac{\mu_0}{\eta}\left(C_0 + \frac{2}{p_2}e^{-p_2d}\right)\right]\Bigg\}\bar{f}(\xi)e^{-i(\zeta+\xi)x}d\xi d\zeta \end{aligned}$$

$$= -\int_{-\infty}^{\infty}\Big[C_{44}\left(p_1B_0 - \frac{s}{2}A_0\right) + p_2\frac{\mu_0}{\eta}C_0 - 2\frac{\mu_0}{\eta}e^{-p_2d} + \epsilon\left(C_{44}p_1B_1 - C_{44}\frac{s}{2}A_1 - i\zeta C_{46}A_1 + p_2\frac{\mu_0}{\eta}C_1\right) - i\zeta C_{46}A_0\Big]e^{-i\zeta x}d\zeta, \quad (30)$$

respectively.

Taking $k = \zeta + \xi$ in the left-hand side of Eqs. (29) and (30) and treating ξ as constant we have $d\zeta = dk$. Substituting $\zeta = k$ in the right-hand side of Eqs. (29) and (30), we get

$$\epsilon R_1(k) = A_0 - C_0 - \frac{2}{p_2}e^{-p_2d} + \epsilon(A_1 - C_1), \quad (31)$$

and,

$$\epsilon R_2(k) = C_{44}\left(-p_1B_0 + \frac{s}{2}A_0 - \epsilon p_1B_1 + \frac{s}{2}\epsilon A_1\right) + ikC_{46}(A_0 + \epsilon A_1) + \frac{\mu_0}{\eta}(2e^{-p_2d} - p_2C_0 - \epsilon p_2C_1) \quad (32)$$

where,

$$R_1(k) = \frac{1}{2\pi}\int_{-\infty}^{\infty}\left[\frac{s}{2}A_0 - p_1B_0 - p_2C_0 + 2e^{-p_2d}\right]^{\zeta=k-\xi}\bar{f}(\xi)e^{-i\xi x}d\xi \quad (33)$$

and,

$$R_2(k) = \frac{1}{2\pi}\int_{-\infty}^{\infty}\Bigg[\Bigg\{C_{44}\left(-A_0p_1^2 - sp_1B_0 + \frac{s^2}{4}A_0\right) - ikC_{46}\left(p_1B_0 - \frac{s}{2}A_0\right) - \frac{\mu_0}{\eta}(C_0p_2^2 + 2p_2e^{-p_2d})\Bigg\} + \Bigg\{i\xi C_{46}\left(p_1B_0 - \frac{s}{2}A_0\right) + k\xi C_{66}A_0 - k\xi\frac{\mu_0}{\eta}\left(C_0 + \frac{2}{p_2}e^{-p_2d}\right)\Bigg\}\Bigg]^{\zeta=k-\xi}\bar{f}(\xi)e^{-i\xi x}d\xi \quad (34)$$

Equating the absolute terms and the coefficient of ϵ in Eqs. (25), (31) and (32), we get

$$A_1\left[C_{44}p_1\sin p_1H - C_{44}\frac{s}{2}\cos p_1H - i\zeta C_{46}\cos p_1z\right] + B_1\left[C_{44}p_1\cos p_1H + C_{44}\frac{s}{2}\sin p_1H + i\zeta C_{46}\sin p_1H\right] = 0, \quad (35)$$

$$A_0\left[C_{44}p_1\sin p_1H - C_{44}\frac{s}{2}\cos p_1H - i\zeta C_{46}\cos p_1H\right] + B_0\left[C_{44}p_1\cos p_1H + C_{44}\frac{s}{2}\sin p_1H + i\zeta C_{46}\sin p_1H\right] = 0, \quad (36)$$

$$A_1 - C_1 = R_1(k), \quad (37)$$

$$A_0 - C_0 = \frac{2}{p_2}e^{-p_2d} \quad (38)$$

$$A_1\left[\frac{s}{2}C_{44} + ikC_{46}\right] - p_1C_{44}B_1 - \frac{\mu_0}{\eta}p_2C_1 = R_2(k), \quad (39)$$

and,

$$A_0\left[\frac{s}{2}C_{44} + ikC_{46}\right] - p_1C_{44}B_0 - \frac{\mu_0}{\eta}p_2C_0 = -2\frac{\mu_0}{\eta}e^{-p_2d}. \quad (40)$$

Solving Eqs. (35) to (40), we get

$$A_0 = \frac{-8\mu_0e^{-p_2d}}{\eta\bar{R}_1(k)}(2p_1C_{44} + sC_{44}\tan p_1H + 2ikC_{46}\tan p_1H) \quad (41)$$

$$B_0 = \frac{8\mu_0e^{-p_2d}}{\eta\bar{R}(k)}(2p_1C_{44}\tan p_1H - sC_{44} - 2ikC_{46}) \quad (42)$$

$$C_0 = -\frac{2e^{-p_2d}}{p_2\bar{R}(k)}\Big(4\frac{\mu_0}{\eta}p_2p_1C_{44} + 2\frac{\mu_0}{\eta}p_2sC_{44}\tan p_1H + 4ik\frac{\mu_0}{\eta}p_2C_{46}\tan p_1 + 4iksC_{44}C_{46}\tan p_1H - 4k^2C_{46}^2\tan p_1H + C_{44}^2s^2\tan p_1H + 4p_1^2C_{44}^2\tan p_1H\Big) \quad (43)$$

$$A_1 = -\frac{2(\mu_0p_2R_1 - R_2)}{\eta\bar{R}(k)}(2p_1C_{44} + sC_{44}\tan p_1H + 2ikC_{46}\tan p_1H),$$

$$B_1 = \frac{2(\mu_0p_2R_1 - R_2)}{\eta\bar{R}(k)}(2p_1C_{44}\tan p_1H - sC_{44} - 2ikC_{46}),$$

$$C_1 = \frac{1}{\bar{R}(k)}(4p_1C_{44}R_2 + 2sC_{44}R_2\tan p_1H + 4ikC_{46}R_2\tan p_1H - 4iskC_{44}C_{46}R_1\tan p_1H + 4k^2C_{46}^2R_1\tan p_1H - s^2C_{44}^2R_1\tan p_1H - 4p_1^2C_{44}^2R_1\tan p_1H) \quad (46)$$

where,

$$\bar{R}(k) = 4iksC_{44}C_{46}\tan p_1H - 4k^2C_{46}^2\tan p_1H - 4ikp_2\frac{\mu_0}{\eta}C_{46}\tan p_1H + s^2C_{44}^2\tan p_1H - 2\frac{\mu_0}{\eta}p_2sC_{44}\tan p_1H - 4\frac{\mu_0}{\eta}p_2p_1C_{44} + 4p_1^2C_{44}^2\tan p_1H. \quad (47)$$

Therefore, the displacement of SH-wave in M_1 layer is given by

$$V_1 = -\frac{1}{2\pi}\int_{-\infty}^{\infty}\frac{8\mu_0 e^{-p_2 d}e^{-\frac{s}{2}z}}{\eta\bar{R}(k)}\left[1 + \frac{\epsilon\left(\frac{\mu_0}{\eta}p_2R_1 - R_2\right)e^{p_2 d}}{4\frac{\mu_0}{\eta}}\right]Ne^{-ikx}dk, \quad (48)$$

where,

$$N = [\cos p_1 z(2p_1C_{44} + sC_{44}\tan p_1H + 2ikC_{46}\tan p_1H) + +\sin p_1 z(2ikC_{46} + sC_{44} - 2p_1C_{44}\tan p_1H)].$$

The Fourier transform of Eq. (1) representing the triangular irregularity at the interface is given by

$$\bar{f}(\xi) = \frac{h}{\epsilon}\int_{-a}^{a}\left(1 - \frac{|x|}{a}\right)e^{i\xi x}dx$$

which on solving gives,

$$\bar{f}(\xi) = \frac{4(1 - \cos(\xi a))}{\xi^2}. \quad (49)$$

Using Eq. (49) in Eqs. (33) and (34), we get

$$\frac{\mu_0}{\eta}p_2R_1 - R_2 = \frac{4\mu_0}{\eta\pi}\int_{-\infty}^{\infty}[\phi(k-\xi) + \phi(k+\xi)]\frac{(1 - \cos(\xi a))}{\xi^2}d\xi \quad (50)$$

where,

$$\begin{aligned}\phi(k-\xi) = \Big[&[-2C_{44}^2s^2p_1p_2 - 8p_1^3C_{44}^2p_2 + 2p_2^2\bar{R}(k) - 2s^2\frac{\mu_0}{\eta}p_2^2C_{44}\tan p_1H \\ &-4iksC_{46}\frac{\mu_0}{\eta}p_2^2\tan p_1H - 8C_{44}p_1^2\frac{\mu_0}{\eta}p_2^2\tan p_1H + 4p_1^2sC_{44}^2p_2\tan p_1H \\ &+8ikC_{46}p_1\frac{\mu_0}{\eta}p_2^2 - 8ikC_{46}C_{44}sp_1p_2 + 4ikC_{46}C_{44}s^2p_2\tan p_1H + s^3C_{44}^2p_2\tan p_1H \\ &-8k\xi C_{46}^2p_1p_2 + 4\xi kC_{46}^2p_2\,\mathrm{s}\tan p_1H + 8ik^2\xi C_{46}C_{66}p_2\tan p_1H + 8k\xi C_{66}C_{44}p_1p_2 \quad (51) \\ &+4k\xi sp_2C_{66}C_{44}\tan p_1H - 4ik^2\xi\frac{\mu_0}{\eta}p_2C_{46}\tan p_1H - 2k\xi s\frac{\mu_0}{\eta}p_2C_{44}\tan p_1H \\ &-4k\xi\frac{\mu_0}{\eta}p_2p_1C_{44} - 4ik^2\xi sC_{44}C_{46}\tan p_1H + \xi k\bar{R}(k) - 4k\xi p_1^2C_{44}^2\tan p_1H \\ &-C_{44}^2s^2k\xi\tan p_1H + 4k^3\xi C_{46}^2\tan p_1H - 4k^2sp_2C_{46}^2\tan p_1H \\ &-2is^2p_2\xi C_{46}C_{44}\tan p_1H + 8k^2p_1p_2C_{46}^2 - 8i\xi C_{46}C_{44}p_1^2p_2\tan p_1H]\frac{e^{-p_2d}}{p_2\bar{R}(k)}\Big]^{\zeta=k-\xi}.\end{aligned}$$

Using the asymptotic formula (Willis, 1948; Tranter, 1966), we have

$$\int_{-\infty}^{\infty}[\phi(k-\xi) + \phi(k+\xi)]\frac{(1 - \cos(\xi a))}{\xi^2}d\xi \cong 2\pi a\phi(k). \quad (52)$$

Using Eq. (52) in Eq. (50), we get

$$\epsilon\frac{\frac{\mu_0}{\eta}p_2R_1 - R_2}{4\frac{\mu_0}{\eta}} = h\phi(k). \quad (53)$$

Using Eq. (53) in Eq. (48), the displacement in the monoclinic layer reduces to

$$\begin{aligned}V_1 &= -\frac{1}{2\pi}\int_{-\infty}^{\infty}\frac{8\mu_0 e^{-p_2d}e^{-\frac{s}{2}z}}{\eta\bar{R}(k)}[1 + h\phi(k)e^{p_2d}]Ne^{-ikx}dk \\ &= -\frac{1}{2\pi}\int_{-\infty}^{\infty}\frac{8\mu_0 e^{-p_2d}e^{-\frac{s}{2}z}}{\eta\bar{R}(k)[1 - h\phi(k)e^{p_2d}]}Ne^{-ikx}dk. \quad (54)\end{aligned}$$

The contribution to the displacement due to dispersion is obtained from the singularities of the integrand of Eq. (54). Thus, the dispersion relation for SH-waves is (Kalyani and Kar, 1986)

$$\bar{R}(k)[1 - h\phi(k)e^{p_2d}] = 0. \quad (55)$$

Substituting $\bar{R}(k)$ and $\phi(k)$ from Eqs. (47) and (51), respectively in Eq. (55), we get

$$\begin{aligned}&4ikC_{44}C_{46}sp_2\tan p_1H - 4k^2p_2C_{46}^2p_2\tan p_1H - 4ikC_{46}p_2^2\frac{\mu_0}{\eta}\tan p_1H \\ &+C_{44}^2s^2p_2\tan p_1H - 2\frac{\mu_0}{\eta}p_2^2sC_{44}\tan p_1H - 4\frac{\mu_0}{\eta}p_2^2p_1C_{44} + 4C_{44}^2p_1^2p_2\tan p_1H \\ &-h[-2C_{44}^2s^2p_1p_2 - 8p_1^3C_{44}^2p_2 + 2p_2^2\bar{R}(k) - 2s^2\frac{\mu_0}{\eta}p_2^2C_{44}\tan p_1H \\ &-4iksC_{46}\frac{\mu_0}{\eta}p_2^2\tan p_1H - 8C_{44}p_1^2\frac{\mu_0}{\eta}p_2^2\tan p_1H + 4p_1^2sC_{44}^2p_2\tan p_1H \quad (56) \\ &+8ikC_{46}p_1\frac{\mu_0}{\eta}p_2^2 - 8ikC_{46}C_{44}sp_1p_2 + 4ikC_{46}C_{44}s^2p_2\tan p_1H \\ &+s^3C_{44}^2p_2\tan p_1H - 4k^2sp_2C_{46}^2\tan p_1H + 8k^2C_{46}^2p_1p_2] = 0\end{aligned}$$

If c denotes the wave velocity of SH-waves propagating along the interface, using Eqs. (12) and (19), we have

$$p_1 = \sqrt{\frac{\omega^2}{\beta_1^2} - \zeta^2 \frac{C_{66}}{C_{44}} + \zeta^2 \frac{C_{46}^2}{C_{44}^2}},\ \ s = -\frac{2i\zeta C_{46}}{C_{44}},\ \ p_2 = \sqrt{\zeta^2 - \eta \frac{\omega^2}{\beta_2'^2}},$$

then, by replacing ζ with k and ω with ck, we obtain

$$p_1 = kP_1,\ \ s = kS,\ \ p_2 = kP_2$$

where

$$P_1 = \sqrt{\frac{c^2}{\beta_1^2} - \frac{C_{66}}{C_{44}} + \frac{C_{46}^2}{C_{44}^2}},\ \ S = -\frac{2iC_{46}}{C_{44}},\ \ P_2 = \sqrt{1 - \eta \frac{c^2}{\beta_2'^2}}.$$

Solving Eq. (56), we get

$$tan\left(kH\sqrt{\frac{c^2}{\beta_1^2} - \frac{C_{66}}{C_{44}} + \frac{C_{46}^2}{C_{44}^2}}\right) = \frac{D_1}{D_2} + i\frac{D_3}{D_4}, \qquad (57)$$

where,

$$D_1 = \left(\frac{\mu_0}{\eta}P_2C_{44} - 2hkC_{44}^2P_1^2 - 2hk\frac{\mu_0}{\eta}C_{44}P_2\right)\left(C_{44}^2 - 2hkC_{44}^2P_2 + 2hkC_{44}\frac{\mu_0}{\eta}P_2\right) + 4h^2k^2P_2\frac{\mu_0}{\eta}C_{46}^2C_{44}$$

$$D_2 = P_1\left(C_{44}^2 - 2hkC_{44}^2P_2 + 2hkC_{44}\frac{\mu_0}{\eta}P_2\right)^2 + 4h^2k^2P_1C_{46}^2C_{44}^2$$

$$D_3 = 2hkC_{46}\frac{\mu_0}{\eta}P_2\left(C_{44}^2 - 2hkC_{44}^2P_2 + 2hkC_{44}\frac{\mu_0}{\eta}P_2\right) - 2hkC_{44}C_{46}\left(\frac{\mu_0}{\eta}P_2C_{44} - 2hkC_{44}^2P_1^2 - 2hk\frac{\mu_0}{\eta}C_{44}P_2\right)$$

$$D_4 = P_1\left(C_{44}^2 - 2hkC_{44}^2P_2 + 2hkC_{44}\frac{\mu_0}{\eta}P_2\right)^2 + 4h^2k^2P_1C_{46}^2C_{44}^2.$$

We now equate the real and imaginary parts on both sides of Eq. (57). We observe that the imaginary part gives $D_3 = 0$, which does not result in the dispersion relation for the governing equation of SH-waves. However, the real part gives the dispersion relation for SH-waves propagating in a monoclinic layer overlying a dry sandy half-space with a triangular irregularity at the interface is given by:

$$tan\left(kH\sqrt{\frac{c^2}{\beta_1^2} - \frac{C_{66}}{C_{44}} + \frac{C_{46}^2}{C_{44}^2}}\right) = \frac{\left(\frac{\mu_0}{\eta}P_2C_{44} - 2hkC_{44}^2P_1^2 - 2hk\frac{\mu_0}{\eta}C_{44}P_2\right)\left(C_{44}^2 - 2hkC_{44}^2P_2 + 2hkC_{44}\frac{\mu_0}{\eta}P_2\right) + 4h^2k^2P_2\frac{\mu_0}{\eta}C_{46}^2C_{44}}{P_1\left(C_{44}^2 - 2hkC_{44}^2P_2 + 2hkC_{44}\frac{\mu_0}{\eta}P_2\right)^2 + 4h^2k^2P_1C_{46}^2C_{44}^2} \qquad \mathbf{(58)}$$

For the existence of pure SH-waves, we consider the range of the dimensionless phase velocity (c/β_1) in Eq. (58) as

$$\sqrt{\frac{C_{66}}{C_{44}} - \frac{C_{46}^2}{C_{44}^2}} < \frac{c}{\beta_1} < \frac{\beta_2'}{\beta_1}.$$

SH-wave propagation in an isotropic layer

From the developed Eq. (58), SH-wave propagation in an isotropic layer overlying an isotropic half-space can be deduced by assuming

$$C_{44} = C_{66} = \mu,\ \ C_{46} = 0,\ \ \eta = 1,\ and\ \ h/H = 0.$$

Thus, Eq. (58) reduces to

$$tan\left(kH\sqrt{\frac{c^2}{\beta_1^2} - 1}\right) = \frac{\mu_0\sqrt{1 - \frac{c^2}{\beta_2'^2}}}{\mu\sqrt{\frac{c^2}{\beta_1^2} - 1}} \qquad (59)$$

Eq. (59) closely matches the well-known established dispersion equation in an isotropic layer overlying isotropic half-space given by Ewing et al. (1957).

NUMERICAL CALCULATION

Having developed the dispersion relation, the effect of triangular irregularity at the interface when the layer is either isotropic or monoclinic and the half-space is with or without sandiness, which have strong influence on the dispersion of the SH-waves, has been studied using the following data (Gubbins, 1990; Pradhan et al., 2023; Madan et al., 2023a)

$$C_{44} = 9.4 \times 10^{10}\ N/m^2, \qquad C_{46} = -1.1 \times 10^{10}\ N/m^2,$$
$$C_{66} = 9.3 \times 10^{10}\ N/m^2, \qquad \mu_0 = 6.54 \times 10^{10}\ N/m^2,$$
$$\rho_1 = 7450\ kg/m^3, \qquad \rho_2 = 3409\ kg/m^3.$$

The results obtained are illustrated graphically in Figures 2-4.

Figure 2 illustrates the dependence of phase velocity (c/β_1) on wave number (kH) in absence of both sandiness $(\eta = 1)$ in the half-space and irregularity $(h/H = 0)$ at the interface, revealing that the phase velocity decreases as the medium of the layer changes from isotropic to monoclinic, showing the influence of monoclinic symmetry (Thomsen, 1986) on wave behaviour and validating the model by comparing it with isotropic results.

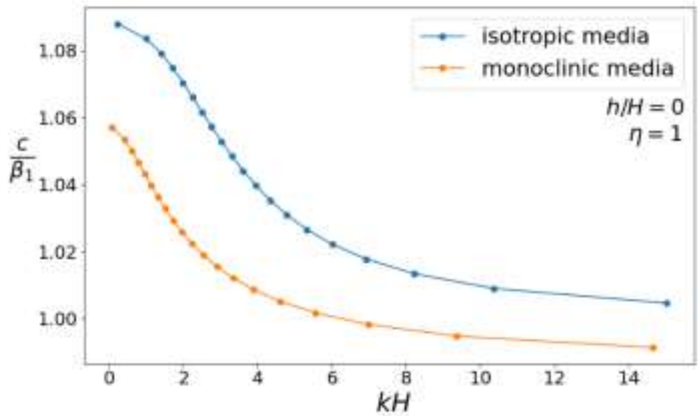

Figure 2. Phase velocity (c/β_1) versus wave number (kH)

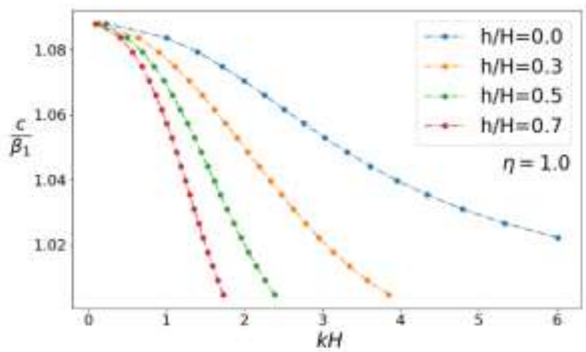

(a) Isotropic layer

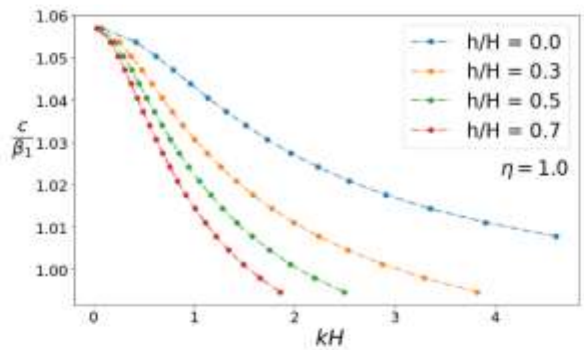

(b) Monoclinic layer

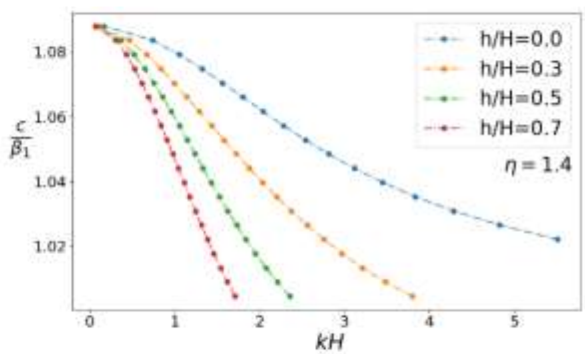

(c) Isotropic layer

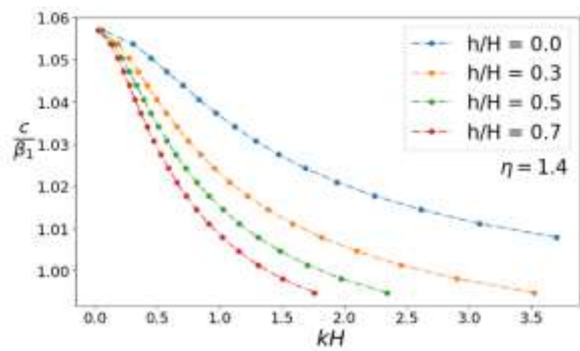

(d) Monoclinic layer

Figure 3. Effect of triangular irregularity, when the layer is (i) isotropic (**a**, **c**), and (ii) monoclinic (**b**, **d**)

Table 2. Variation of phase velocity with depth of triangular irregularity for isotropic and monoclinic media

Depth of triangular irregularity	$\eta = 1, kH = 1$		$\eta = 1.4, kH = 1$	
	c/β_1 in isotropic medium	c/β_1 in monoclinic medium	c/β_1 in isotropic medium	c/β_1 in monoclinic medium
$h/H = 0$	1.083	1.043	1.088	1.037
$h/H = 0.3$	1.077	1.030	1.070	1.023
$h/H = 0.5$	1.069	1.022	1.060	1.015
$h/H = 0.7$	1.058	1.014	1.047	1.008

In the absence of sandiness ($\eta = 1$) in the half-space, Figures 3(a) and 3(b) depict the variation in phase velocity with wave number in isotropic and monoclinic media respectively for different values of the depth of triangular irregularity. From these figures, it is observed that the phase velocity decreases as the depth of triangular irregularity increases in both media, which is consistent with the observations by Chattopadhyay et al. (2008) and Madan et al. (2024), where similar results were observed. Further, in the presence of sandiness ($\eta = 1.4$), Figures 3(c) and 3(d) depict the variation in phase velocity with wave number in isotropic and monoclinic media, respectively, for different values of the depth of triangular irregularity. Similar trends of decreasing phase velocity with increasing depth of triangular irregularity are observed in these figures. Moreover, it is noteworthy from Table 2 that when the layer changes from isotropic to monoclinic, the phase velocity decreases by approximately 4% in both the presence and absence of sandiness.

Figures 4(a) and 4(b) depict the variation of dimensionless phase velocity with dimensionless wave number for isotropic and monoclinic media, respectively, without irregularity at the interface ($h/H = 0$). These figures indicate that as the sandiness parameter increases from $\eta = 1$ to $\eta = 1.4$, the phase velocity decreases for both media. It is also observed from Table 3 that, at kH equals to 4, the phase velocity decreases as the medium of the layer changes from isotropic to monoclinic.

Further, in the presence of a triangular irregularity ($h/H = 0.4$) and the layer is either isotropic or monoclinic, it is observed from Figures 4(c) and 4(d) that the phase velocity decreases as the wave number increases for all values of the sandiness parameter. From Table 3, similar trends are also observed at kH equals to 1.5, where the phase velocity in the monoclinic medium is lower than that in the isotropic medium.

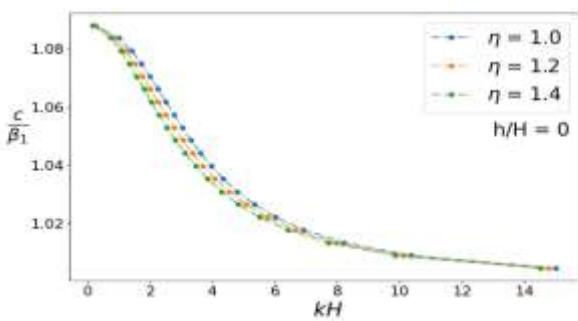

(a) Isotropic layer

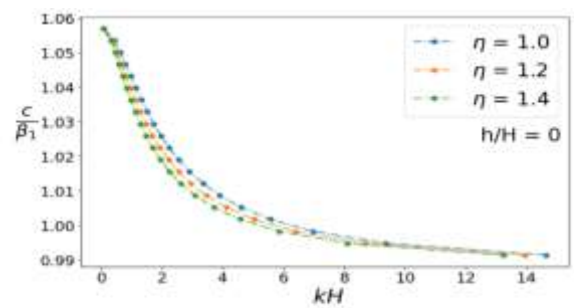

(b) Monoclinic layer

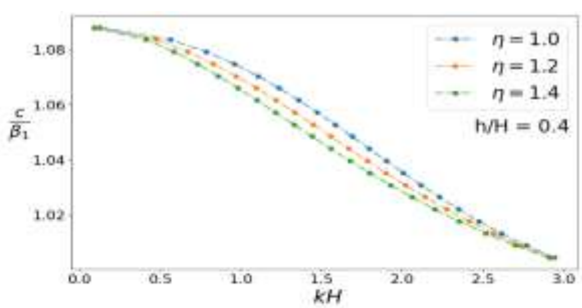

(c) Isotropic layer

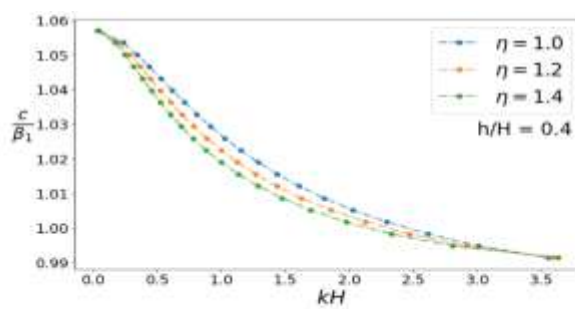

(d) Monoclinic layer

Figure 4. Effect of sandiness, when the layer is (i) isotropic (**a**, **c**), and (ii) monoclinic (**b**, **d**)

Table 3. Variation of phase velocity with sandiness parameter for isotropic and monoclinic media

Sandiness parameter	$h/H = 0, kH = 4$		$h/H = 0.4, kH = 1.5$	
	c/β_1 in isotropic medium	c/β_1 in monoclinic medium	c/β_1 in isotropic medium	c/β_1 in monoclinic medium
$\eta = 1$	1.039	1.008	1.056	1.014
$\eta = 1.2$	1.036	1.006	1.050	1.010
$\eta = 1.4$	1.033	1.004	1.046	1.008

CONCLUSIONS

This study investigates the influence of a triangular irregularity on the dispersion characteristics of SH-waves propagating in a monoclinic crustal layer overlying a dry sandy half-space. The analysis considers variations in sandiness in the half-space and in the depth of interface irregularity. Further, monoclinic and isotropic media are compared to show the impact of symmetry on wave behaviour and validate the developed model in the present study. Our findings enhance the understanding of SH-wave propagation in complex geological settings and offer practical implications for geophysical exploration and engineering applications involving layered, anisotropic, and heterogeneous subsurface structures. The highlights of the findings of this study are given below:

1. SH-waves exhibit dispersive behaviour in the monoclinic medium, as the phase velocity varies with wave number and converges at different values depending on the material properties.
2. The phase velocity of SH-waves is hindered in the monoclinic medium, showing a decreasing trend with increasing wave number.
3. The transition of the layer medium from isotropic to monoclinic, results in a consistent decrease in phase velocity regardless of the presence of sandiness or interface irregularity.
4. An increase in the depth of triangular irregularity at the interface leads to a reduction in phase velocity for both isotropic and monoclinic media, independent of the sandiness in the half-space.
5. An increase in the sandiness parameter of the half-space reduces the phase velocity in both types of media, irrespective of whether the interface is smooth or irregular.

ACKNOWLEDGMENT

The author, Tanishqa Shivaji Veer, gratefully acknowledges the financial assistance provided by Dr. Vishwanath Karad MIT World Peace University, Pune-411038, Maharashtra, India, through a Junior Research Fellowship. The authors express their gratitude to Dr. O. P. Pandey, the Chief Editor, for his insightful feedback and for editing the final manuscript. The authors are also thankful to reviewers for their comments and suggestions in the improvement of the manuscript.

Author Credit Statement

All authors have contributed equally. All authors have read and approved the manuscript.

Data availability

No data were used in this study.

Compliance with ethical standards

Authors declare no conflict of interest and adhere to copyright norms.

REFERENCES

Acharya, D. P. and Roy, I., 2009. Effect of surface stress and irregularity of the interface on the propagation of SH-waves in the magneto-elastic crustal layer based on a solid semi space. Sādhanā, 34, 309-330.

Chattopadhyay, A., 1975. On the dispersion equation for Love waves due to irregularity in the thickness of the non-homogeneous crustal layer. Acta Geophys. Polonica, 23, 307-317.

Chattopadhyay, A. and De, R. K., 1983. Love type waves in a porous layer with irregular interface. Int. J. Eng. Sci., 21(11), 1295-1303.

Chattopadhyay, A. and Saha, S., 1996. Reflection and refraction of P waves at the interface of two monoclinic media. Int. J. Eng. Sci., 34(11), 1271-1284.

Chattopadhyay, A., Gupta, S., Sharma, V. K. and Kumari, P., 2008. Propagation of SH waves in an irregular monoclinic crustal layer. Arch. Appl. Mech., 78, 989-999.

Ewing, M., Jardetzky, W. and Press, F., 1957. Elastic Waves in Layered Media. McGraw-Hill, New York.

Gubbins, D. 1990., Seismology and plate tectonics. Cambridge University Press, Cambridge.

Gupta, S., Das, S. K. and Pramanik, S., 2021. Impact of irregularity, initial stress, porosity, and corrugation on the propagation of SH wave. Int. J. Geomech., 21(2), 04020245.

Kalyani, V. K. and Kar, B. K., 1986. Propagation of Love waves in an irregular anisotropic porous layer sandwiched between two homogeneous half-spaces. Gerlands Beilr. Geophys, 95(1), 27-35.

Kalyani, V. K., Sinha, A., Pallavika, Chakraborty, S. K. and Mahanti, N. C., 2008. Finite difference modeling of seismic wave propagation in monoclinic media. Acta Geophys., 56, 1074-1089.

Kar, B. K., Pal, A. K. and Kalyani, V. K., 1986. Propagation of Love waves in an irregular dry sandy layer. Acta Geophys. Polonica, 34(2), 157-170.

Kaur, J. and Tomar, S. K., 2004. Reflection and refraction of SH-waves at a corrugated interface between two monoclinic elastic half-spaces. Int. J. Numer. Anal. Methods Geomech., 28(15), 1543-1575.

Khan, A. A., Dilshad, A., Rahimi-Gorji, M. and Alam, M. M., 2021. Effect of initial stress on an SH wave in a monoclinic layer over a heterogeneous monoclinic half-space. Math., 9(24), 3243.

Kreyszig, E., 2006. Advanced Engineering Mathematics. John Wiley and Sons, New Jersey, 9th edition.

Kumar, N. and Madan, D. K., 2022. Propagation of love waves in dry sandy medium laying over orthotropic semi-infinite medium with irregular interface. AIP Conf. Proc., 2481(1), 040019.

Kumar, R., Madan, D. K. and Sikka, J. S., 2015. Effect of irregularity and inhomogeneity on the propagation of Love waves in fluid saturated porous isotropic layer. J. Appl. Sci. Techno., 20, 16-21.

Madan, D. K., Kumar, N. and Goyal, R., 2023a. SH wave propagation in dry sandy media overlying an orthotropic elastic layer and a pre-stressed dry sandy half-space. Punjab Univ. J. Math., 55(8), 327-342.

Madan, D. K., Kumar, N. and Rani, A. 2023b. Rayleigh wave propagation in isotropic sandy layer sliding over isotropic

sandy semi-infinite medium with sliding contact. Int. J. Appl. Mech. Eng., 28(1), 58-70.
Madan, D. K., Kumar, N. and Muwal, R. 2024., Dispersion of Love wave in a viscoelastic sandy layer overlying anisotropic half-space with parabolic interface. Jñānābha, 54(1), 244-253.
Nye, J. F., 1985. Physical Properties of Crystals: Their Representation by Tensors and Matrices. Oxford University Press, Oxford, New York.
Pal, A. K., 1985. The propagation of Love waves in a dry sandy layer. Acta Geophys. Polonica, 33(2), 183–188.
Pal, P., Majhi, S. and Kumar, S., 2016. Propagation of SH-waves in a sandwiched dry sandy medium. Conference GSI, 70–73.
Pilant, W. L., 1979. Elastic Waves in the Earth (Developments in Solid Earth Geophysics). Elsevier, Holland.
Pradhan, N., Manna, S. and Samal, S. K., 2023. SH-type wave motion in a geophysical model with monoclinic and heterogeneous media due to a point source at the interface. Arch. Appl. Mech., 93, 2613-2629.
Pradhan, N., Manna, S., Samal, S. K. and Saha, S., 2025. SH-wave in two-layered structure of functionally graded viscoelastic and monoclinic media under the influence of an interior point source. Eur. Phys. J. Plus, 140, 181.
Sethi, M. and Sharma, A., 2016. Propagation of SH waves in a regular non-homogeneous monoclinic crustal layer lying over a non-homogeneous semi-infinite medium. Int. J. Appl. Mech. Eng., 21(2), 447–459.
Thomsen, L., 1986. Weak elastic anisotropy. Geophys., 51(10), 1954-1966.
Tomar, S. K. and Kaur, J., 2007. SH-waves at a corrugated interface between a dry sandy half space and an anisotropic elastic half-space. Acta Mech., 190, 1–28.
Tranter, C. J., 1966. Integral Transform in Mathematical Physics. Methuen and Co. Ltd., London.
Willis, H. F., 1948. LV. A formula for expanding an integral as a series. London Edinburgh Philos. Mag. & J. Sci., 39(293), 455–459.

Received on: 25-06-2025; Revised on: 19-08-2025; Accepted on: 21-08-2025